Revision

30th August 2013

Liquid | Liquid Interfacial Photoelectrochemistry of Chromoionophore I Immobilised in 4-(3-Phenylpropyl)-Pyridine Microdroplets

Thomas R. Bartlett [a], Safeer Ahmed [a,b], Floriana Tuna [c], David Collison [c], Gary J. Blanchard [d], and Frank Marken* [a]

[a] *Department of Chemistry, University of Bath, Claverton Down, Bath BA2 7AY, UK*

[b] *Department of Chemistry, Quaid-i-Azam University,45320 Islamabad, Pakistan.*

[c] *School of Chemistry, The University of Manchester, Oxford Road, Manchester M13 9PL, UK*

[d] *Michigan State University, Department of Chemistry, East Lansing, Michigan 48824-1322 USA*

To be submitted to ChemElectroChem

Proofs to F. Marken

Email f.marken@bath.ac.uk

Abstract

Photoelectrochemical processes are investigated for chromoionophore I (ETH 5294) dissolved in 4-(3-phenylpropyl)-pyridine (or PPP) and deposited in the form of a micro-droplet array (via evaporation deposition from an acetonitrile solution) onto a 5 mm diameter basal plane pyrolytic graphite (BPPG) electrode. Stable biphasic dark voltammetric responses (2-electron 2-proton) are observed in phosphate buffer solution (from pH 2 to pH 12) with a switch in reactivity at pH 5 due to a biphasic protonation step. Photo-electrochemical activity at pH 2 is investigated further by photo-transient amperometry. The protonated chromoionophore I is shown to be the photo-active component (supported by EPR data) and "hole-transfer" at the liquid | liquid interface to aqueous oxalate is demonstrated. This interfacial hole-transfer process can be "switched off" by hydrophobic anions (PF_6^-) competing for cationic liquid | liquid PPP surface binding sites. Implications for light harvesting and liquid semiconductor properties are discussed.

Keywords: chromoionophore, ETH 5294, voltammetry, ion transfer, liquid | liquid interface, triple phase boundary, photoelectrochemistry, semiconductor.

Introduction

Chromoionphore I (or ETH 5294, see structure in Figure 1A) has been used as transmissive or fluorescent probe molecule in many types of hydrophobic sensor membranes, for example for sensing H^+ [1,2,3], Li^+ [4], K^+ [5], nitrite [6], surfactants [7], or for Hg(II) [8]. Chromoionophore I is usually employed in PVC membranes but has also been shown to respond to acids in ionic liquids [9]. This versatile range of sensing applications is based on the optical response to proton or ion transfer, for example for Hg(II) detection. Corresponding detection methods based on microspheres [10,11] and micro-optical sensors [12] have been developed. Chromoionophore I has been used in optode membranes for pH [13], and in optical wave-guide bio-sensor applications [14], for example for urea determination. Sol-gel sensor structures with chromoionophor I [15] have been demonstrated. Chromoionophore I diffusion has been investigated by potential step [16] and potentiometry methods [17] at membranes. However, electrochemical or photo-electrochemical properties of chromoionophore I have previously not been reported. It is shown here that chromoionophore I exhibits a well-defined biphasic redox transition and protonation (corresponding to the well-known optical transition used in sensing) with a shift in reversible potential indicating the biphasic protonation process [18]. Furthermore, chromoionophor I dissolved in 4-(3-phenylpropyl)-pyridine is shown to be photo-electrochemically active. In the excited state charge separation and liquid | liquid interfacial hole-quenching by aqueous oxalate is reported.

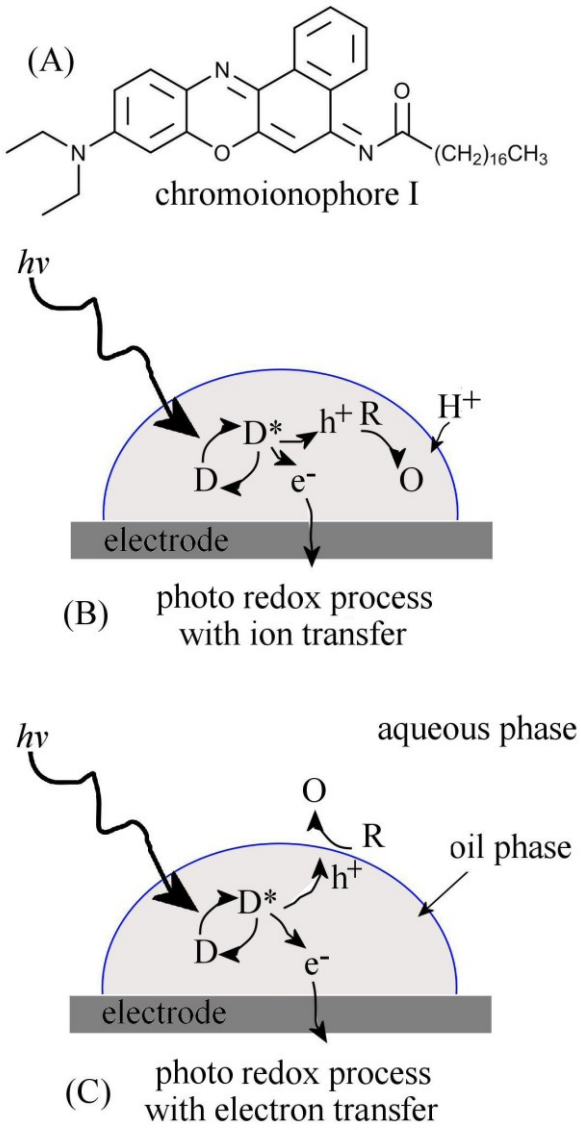

Figure 1. (A) Molecular structure of oil-soluble dye chromoionophore I (or ETH 5294). (B) Schematic diagram of the photochemical reaction sequence with a redox process coupled to ion transfer. (C) Schematic diagram of the photochemical reaction sequence with a redox process coupled to electron transfer.

Work on both triple phase boundary ion transfer processes [19,20] and photo-electrochemical processes [21,22,23] started with phenylenediamine derivatives. In previous reports photo-electrochemical processes in microdroplet media (or under triple phase boundary conditions [24]) were found to occur within the organic phase

(coupled to interfacial ion transfer) via photo-comproportionation [25] or with added duroquinol reagents [26] (see Figure 1B). However, in order to extract redox energy from photo-electrochemical processes it is necessary for "hole-transfer" to happen across the liquid | liquid phase boundary (see Figure 1C). This report provides initial evidence for a liquid | liquid hole transfer from a photo-excited state within the oil phase to the aqueous oxalate quencher anion. This reaction is proposed to occur within the oil-aqueous interfacial double layer. It is demonstrated that this process is suppressed by interfacial cation site blocking, for example by addition of hydrophobic PF_6^- into the aqueous phase. Implications for future photo-electrochemistry and energy harvesting processes at "soft interfaces" are discussed.

Results and Discussion

Dark Voltammetry of Chromoionophore I in 4-(3-Phenyl-propyl)-pyridine

Chromoionophore I (or ETH 5294) is a Nile blue-type dye made hydrophobic by an amide group with hydrophobic tail (see Figure 1A). The electrochemistry of amide-derivatised Nile blues has been reported [27] and the general mechanism for Nile blue (a phenoxazine mediator) reduction has been shown to follow a 2-electron pathway [28,29]. Chromoionophore I dissolved in 4-(3-phenyl-propyl)-pyridine (PPP) and immobilised on graphite (BPPG) in the form of microdroplets shows similar electrochemical characteristics when immersed into aqueous buffer solution. Figure 2A shows typical voltammograms obtained at different scan rates in 0.5 M phosphate buffer at pH 2. The reduction at 0.1 V vs. SCE is associated with a corresponding

oxidation indicating overall chemical reversibility. The voltammetric signal is stable over prolonged potential cycling due to insignificant losses of the hydrophobic dye into the aqueous phase.

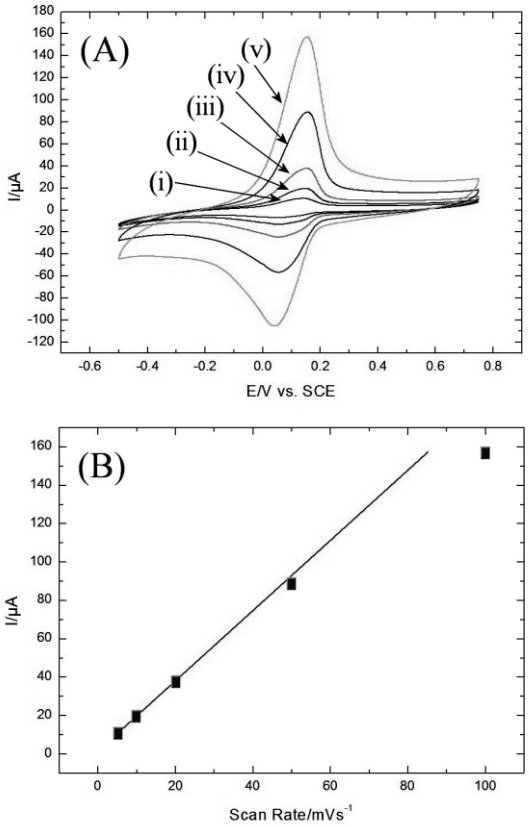

Figure 2. (A) Cyclic voltammograms (scan rate 5, 10, 20, 50, and 100 mVs^{-1}) of a 40 nL deposit of 42 mM chromoionophore I/PPP micro-droplets on BPPG immersed in 0.5 M phosphate buffer pH 2. (B) Plot of anodic peak current versus scan rate showing linear dependence at lower scan rate.

When investigated over a range of scan rates, a linear dependency of peak current versus scan rate is observed (Figure 2B) indicative of rapid transport within small microdroplets. The effect of pH on the chemically reversible chromoionophore I reduction is investigated next. A shift of the voltammetric response due to involvement of protons in the reduction is observed as well as a more subtle and

complicated change in peak shape (see Figure 3A).

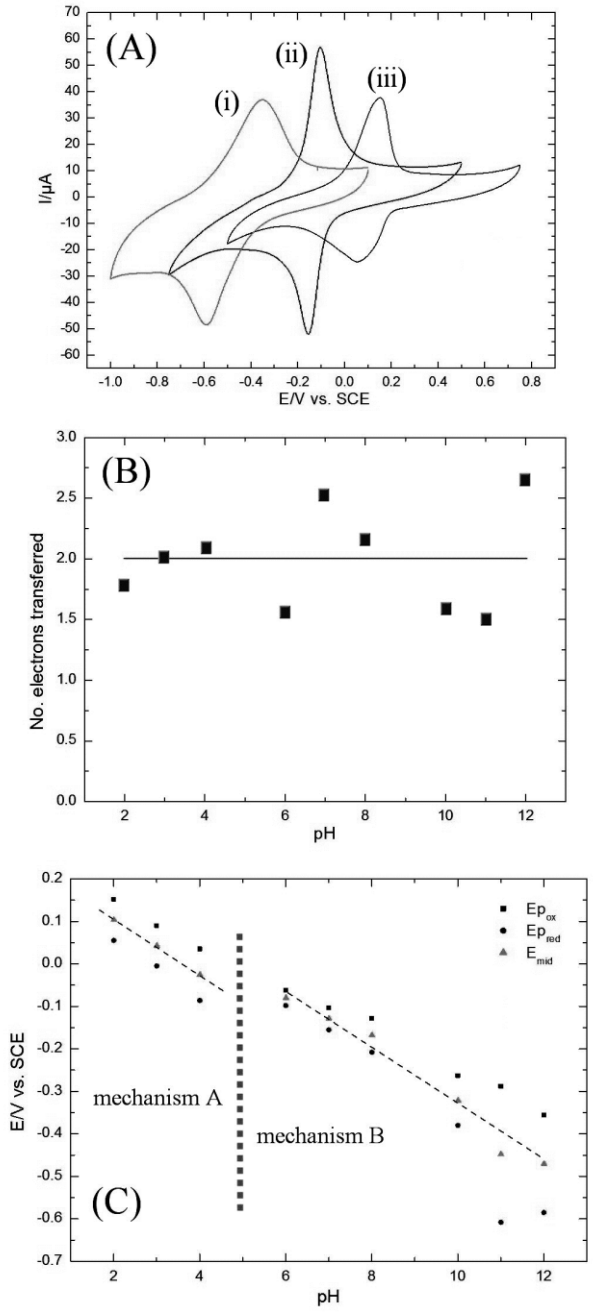

Figure 3. (A) Cyclic voltammogram (scan rate 20 mVs^{-1}) for a 40 nL deposit of 42 mM chromoionophore I/PPP on BPPG immersed in 0.5 M phosphate buffer (i) pH 4, (ii) pH 7, and (iii) pH 12. (B) Plot of the number of electrons transferred per molecule during oxidation (at 20 mVs^{-1}; obtained by integration of the anodic peak) versus pH indicative of a 2-electron mechanism across the pH range. (C) Plot of anodic and cathodic peak potentials and midpoint potential (scan rate 20 mVs^{-1}) versus pH.

A plot of the charge under the reduction or oxidation peak versus pH, or a plot of the corresponding number of electrons transferred per chromoionophore I molecule immobilised at the electrode surface (see Figure 3B) is consistent with a 2-electron mechanism over the entire pH range studied here. Therefore mechanism A (acidic range, see Figure 3C) can be described by equation 1.

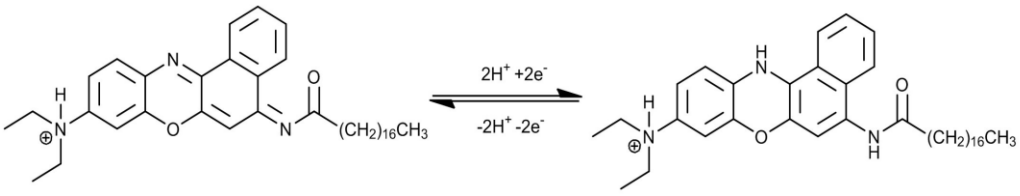

(1)

Here, the protonated form of the oxidised dye is reduced to the protonated leuco-form of chromoionophore I. In contrast, under more alkaline conditions mechanism B (basic range, see Figure 3C) is operative (equation 2).

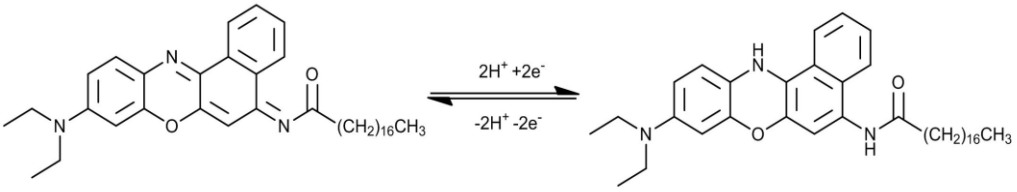

(2)

The transition from mechanism A to B occurs at approximately pH 5 (consistent with the colour change exploited in optical sensor applications, *vide supra*) in phosphate buffer, but the transition point is sensitive to the presence of more hydrophobic anions (similar to processes in optical sensor membranes [12] and similar to related biphasic protonation mechanisms for ferrocene redox systems [18]). The additional

broadening of both reduction and oxidation peaks and the widening of the peak-to-peak separation at more alkaline pH have been attributed to a change at the PPP – water liquid | liquid interface as described previously for the pentoxyresorufin dye system [26]. Additional variability of shape and magnitude of voltammetric responses (see Figure 3B) is mainly due to the random nature of the microdroplet formation by solvent evaporation.

Photo-Voltammetry of Chromoionophore I in 4-(3-Phenyl-propyl)-pyridine (or PPP)

Photoelectrochemical responses were studied initially with pulsed light from a halogen lamp (see Experimental) applied during cyclic voltammetry. Figure 4A shows typical data. The black curve was obtained without pulsed light and the red voltammogram shows the effect of light pulses. Photo-responses are weak but occur at potentials positive of 0.1 V vs. SCE. That is, the oxidised form of the chromoionophore I dye is photochemically active and the reduced leuco-chromoionophore I (with the LUMO filled) is photochemcially inactive. The experiment was repeated after addition of 10 mM KPF_6 into the aqueous electrolyte to explore the effect of hydrophobic anions (not shown). Only insignificant changes in both the shape of the cyclic voltammogram and the photo-responses were observed (a decrease in the photo-response occurs, vide infra). Therefore anion transfer at the liquid|liquid interface appears not to be important as part of both the overall dark or the photo-electrochemical mechanism. Additional survey experiments at pH 7 and pH 12 (not shown) revealed that the most clear photo-current responses are observed at

pH 2, which was therefore selected for further study.

Next, photo-current transients were recorded in chronoamperometry mode at fixed potential of 0.4 V vs. SCE. Figure 4B and 4C show photo-current transients reminiscent of those usually seen at semiconductor electrodes [30]. The light-on transient is linked to a peak followed by current decay into a photo-stationary current signal (anodic). The light-off transient shows a cathodic peak followed by return to equilibrium current conditions. The peak transients are likely to be associated with charge carrier mobility effects and the development of concentration gradients in the microdroplet phase (rather than charging of a static space-charge region as seen in solid bulk semiconductors [30,31]). The initial peak in the light-on transient can be interpreted tentatively in terms of holes reaching the electrode surface first and causing an anodic peak [30] consistent with a faster apparent "hole" diffusion relative to "electron" diffusion ($D_{hole} > D_{electron}$). The decay of current towards the photo-stationary state would then be linked to the establishment of electron and hole concentration gradients within microdroplets. Contributions to these apparent diffusion rates may arise here from "hole hopping" for example via chromoionophor I collisions or via PPP solvent molecules. The extent of the "active" reaction zone in microdroplets is currently not known. Also, the molecular mechanism and products for these photo-processes in the absence of quenchers such as oxalate (*vide infra*) are currently unknown.

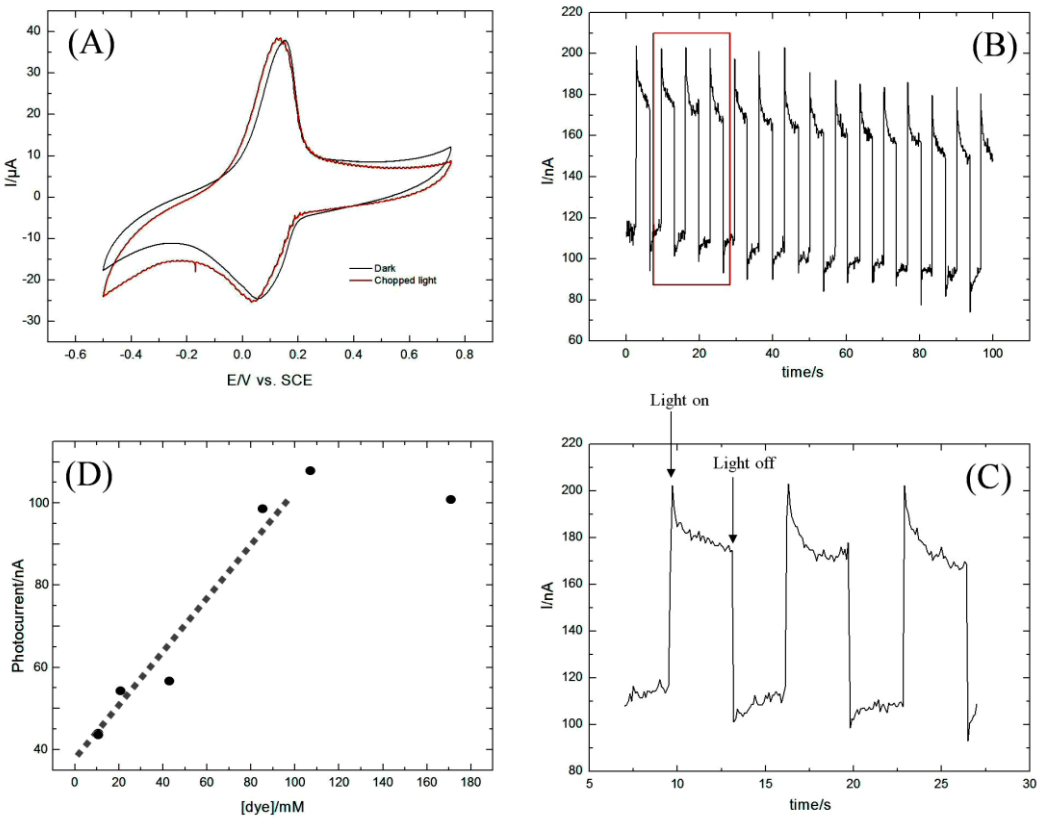

Figure 4. (A) Cyclic voltammogram (scan rate 20 mVs^{-1}) of 42 mM chromoionophore I/PPP (40 nL) micro-droplets under dark conditions (black) and in chopped light (red) in 0.5 M phosphate buffer pH 2. (B) Chronoamperometry for 42 mM chromoionophore I/PPP (40 nL) micro-droplets, at 0.4 V vs. SCE under chopped light conditions at pH 2. (C) Enlargement of photocurrent transients. (D) Plot of photo-transient current versus chromoionophore I concentration (40 nL PPP).

The concentration of the chromoionophore dye has a strong effect on the photocurrent as shown in Figure 4D. An almost linear increase is observed indicative of a direct link of Beer-Lambert light absorption by the dye in the microdroplet to the resulting photo-transient responses. Further evidence for the nature of the photo-excited species is obtained from "action spectrum" analysis. Figure 5A shows UV/Vis absorption data for chromoionophore I in PPP (i) non-protonated and (ii) protonated. These spectral data are in good agreement with UV/Vis data reported previously in other organic solvent or membrane systems [8].

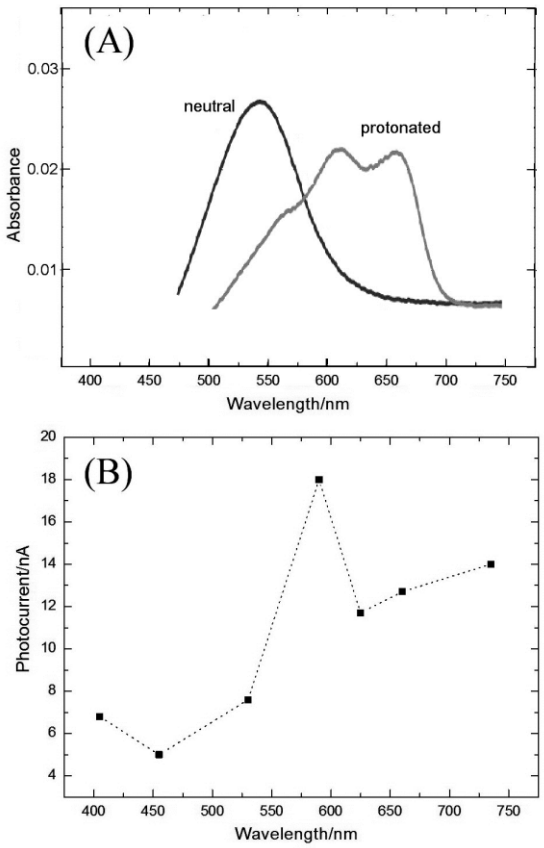

Figure 5. (A) UV/Vis absorbance spectra of 8.6 μM chronoionophore I in PPP (neutral and protonated with 0.01 M $HClO_4$). (B) "Action plot" of photocurrent versus LED wavelength for pulsed-light chronoamperometry for a deposit of 42 mM chromoionophore I/PPP (40 nL) micro-droplets on BPPG at 0.4 V vs. SCE at pH 2 (in 0.5 M phosphate buffer). LED sources were maintained at a constant intensity across the range of wavelengths.

Action spectra were obtained with a set of LEDs with approximately equal intensity (calibrated with a photodiode) to cover the range of wavelengths. Figure 5B shows a plot of the photo-transient current response plotted versus the wavelength. A clear maximum is observed at approximately 580 nm, which is in excellent agreement with the absorption band of the protonated chromoionophore I (compare to Figure 5A). Therefore this has to be regarded as the main photo-active component under these conditions.

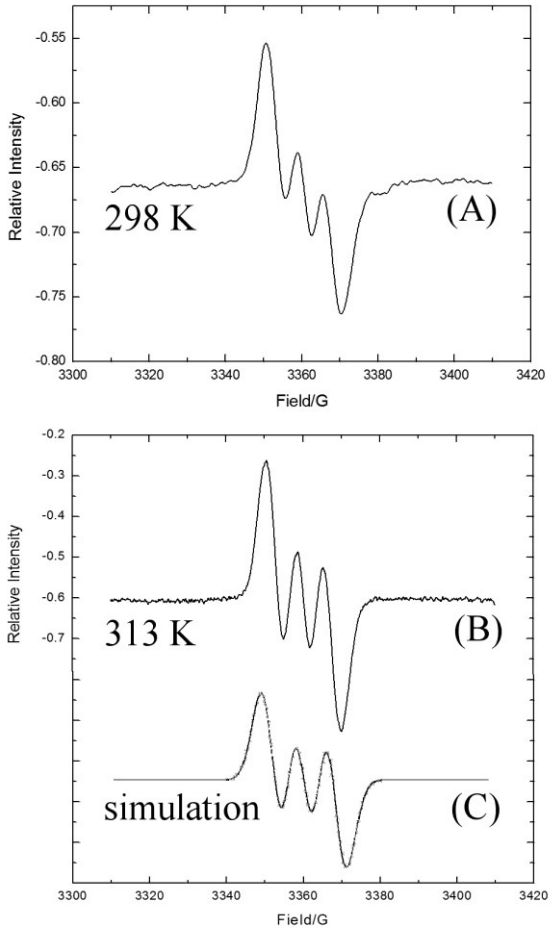

Figure 6. (A) Room temperature EPR spectrum for protonated chromoionophore I (ca. 1 mM dissolved in PPP with 10 mM $HClO_4$) when exposed to light (white halogen light source). (B) Elevated temperature EPR for the same sample. (C) Approximate simulation (SimFonia, Bruker) based on hyperfine interaction to one N (8 G) and one H (2 G) and a line-width of 6 G.

Additional evidence for the presence of long-lived photo-excited intermediates comes from electron paramagnetic resonance (EPR) measurements. When a halogen light (see experimental) is switched on, a clear signal for a paramagnetic species is observed. Time transients for light-on light-off transients (not shown) clearly link the signal to the presence of light. In order to better resolve spectral features the

temperature was increased to 313 K (see Figure 6B), but only two hyperfine coupling constants estimated as 8 G (N) and 2 G (H) are revealed. The chemical nature of the radical species is therefore currently not fully resolved.

Photo-Voltammetry of Chromoionophore I in 4-(3-Phenyl-propyl)-pyridine Immersed in Aqueous Oxalate

Although evidence for the photo-electrochemical chromoionophore I process is strong, there is so far no overall mechanism identifying the products of the photo-anodic process. In order to clearly associate a "hole-quenching" process at the liquid | liquid interface with the photo-process further experiments were performed in the presence of oxalate anions in the aqueous phase as well-known sacrificial hole-quencher [32]. In acidic media the process involves irreversible formation of CO_2. Oxalic acid has pK_A values of 4.19 and 1.23 at 25 ^oC [33] and therefore exists predominantly as the mono-anion in aqueous phosphate buffer at pH 2.

Typical photo-current transients without and with 4 mM oxalate are shown in Figure 7A and 7B, respectively. A significant increase in the photocurrent in the presence of oxalate suggests effective hole quenching at the liquid | liquid interface. Photo-currents increase significantly with oxalate concentration and then plateau at an aqueous oxalate concentration of approximately 40 mM. A step in the data at about 4 mM appears reproducibly and may be associated with localised CO_2 gas bubble formation at the triple phase boundary (see Figure 7C). Most strikingly, the presence of a competing hydrophobic anion, such as PF_6^-, causes a complete loss of photo-

activity (see Figure 7C). This phenomenon could be interpreted as a competition for liquid | liquid interfacial binding sites (protonated PPP), where hydrophobic PF_6^- blocks the interaction of hydrophilic oxalate with the positively charged PPP oil-water interface [26] and thereby stops the interfacial hole quenching process. In addition, the PF_6^- could cause depolarisation of the liquid|liquid interface. Therefore efficient photo-currents appear to be strongly dependent on the binding interaction of the hole quencher with the interface. In future, appropriate molecular hole-quenching systems need to be developed to not only dissipate the energy (as with oxalate), but to transport redox energy across the aqueous phase into a suitable counter/collector electrode.

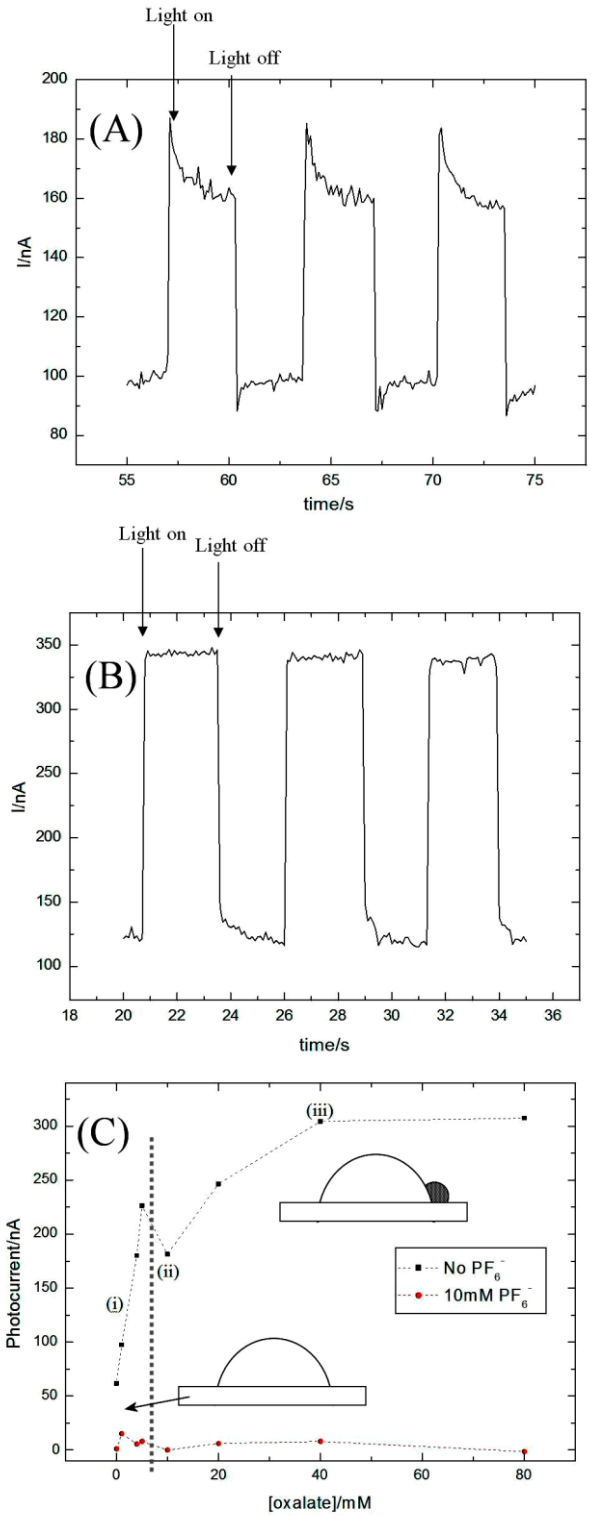

Figure 7. (A) Chronoamperometry data (chopped light, halogen source) for 42 mM chromoionophore I/PPP (40 nL) micro-droplets on BPPG at 0.4 V vs. SCE immersed in 0.5 M phosphate buffer at pH 2. (B) As above with 4 mM oxalate. (C) Plot of photocurrent versus oxalate concentration for phosphate buffer solutions containing no $NaPF_6$ (black) and with 10 mM $NaPF_6$ (red). Inserts shows a schematic representation of CO_2 bubble formation in the triple phase boundary region with onset at 4 mM oxalate.

Conclusions

Chromoionophore I voltammetry in the dark and under biphasic (micro-droplet) conditions has been reported and the pH dependence has been shown to reveal a similar "switch" behaviour as that exploited in optical membrane sensing systems. The hydrophobic chromoionophore I molecule provided a highly stable and reproducible 2-electron 2-proton redox system in the oil phase with a midpoint potential indicative of the aqueous solution pH.

Chromoionophore I has been shown to be also photo-electrochemically active in PPP – aqueous biphasic environments. Weak, but clear photo-responses were observed and shown to be associated with the protonated chromoionophore I. In the presence of oxalate hole-quencher in the aqueous phase, clear evidence for an interfacial hole-transfer was obtained and new insights into the conditions during the hole-transfer were obtained. The role of competing hydrophobic anion, here PF_6^-, in particular shows that the interaction of the quencher with the liquid | liquid interface is crucial for energy harvesting. Important questions such as those concerning the type of species involved in the photo-process and the concentration profiles for "electrons" and "holes" in microdroplets as well as liquid | liquid interfacial reactivity [34] remain open. Further comparison with literature reports on known photo-processes in polymer structures [35] and in novel graphene-based materials [36] will be necessary. In future, liquid | liquid interface processes mimicking biological photosynthesis could be experimentally accessible via triple phase boundary photo-voltammetry and

a wider range of systems including cases of interfacial hydrogen and oxygen formation will be subjected to study or screening to reveal the kinetic and thermodynamic features that are important in these light energy harvesting processes.

Experimental

Chemicals and Reagents

Chromoionophore I (ETH 5294, Aldrich), 4-3(3-phenylpropyl)-pyridine (PPP) (Aldich, 97%), acetronitrile (Aldrich, Reagent Plus), sodium hydroxide (Aldrich, >97%), orthophosphoric acid (Fischer Scientific, 85 wt%), sodium hexafluorophosphate (Aldrich, 98%), oxalic acid (Aldrich, 98%), perchloric acid (Aldrich, 70%) were obtained commercially and used without further purification. A Thermo Scientific purification device was used to provide filtered, demineralised water with resistivity of >18.2 MΩcm. The laboratory temperature was 20 ^{o}C ± 2 ^{o}C.

Instrumentation

A μAUTOLAB Type II potentiostat (Metrohm, Netherlands) was used for all voltammetric measurements. Photo-electrochemical action spectra were obtained with a set of LEDs (Thorlabs, UK) and an Ivium Technologies Compactstat potentiostat. A standard three-electrode electrochemical glass cell was used, using a flat bottomed 100 cm^3 flask to allow light to be directed up through the cell on to the electrode. The working electrode used was a basal plane pyrolytic graphite (BPPG) electrode with a diameter of 5 mm, mounted in a Teflon sheath, coated with oil microdroplets, and submerged into the aqueous phosphate buffer solution. The counter electrode was a platinum wire, and the reference electrode was a saturated calomel (SCE) electrode.

Phosphate buffer pH was measured with a JENWAY 3505 pH meter.

The light source used for photochemical investigations was a Fiber-Lite high intensity halogen bulb (MI-150) (Dollan-Jenner Industries), with an intensity of approx. 16.5 $mWcm^{-2}$ at the electrode surface. Light intensity measurements were conducted with a Thorlabs optical power meter (PM100A). Chopping of the light was conducted manually. For variable wavelength experiments the following Thorlabs mounted high power LED light sources were used: M405L2, M455L2, M530L2, M590L2, M625L2, M660L3, M735L3. LED sources were maintained at a constant intensity of approx. 50 mW cm^{-2} and pulsed using a Function/Arbitrary generator TG4001. UV/Vis spectroscopy was conducted using a Perkin-Elmer Lambda 40 spectrometer in 1 mm pathlength quartz cells. Electron paramagnetic resonance (EPR) spectra were obtained on a Bruker EMXmicro spectrometer (X-band) with nitrogen gas flow temperature control and sample illumination with a Fiber-Lite high intensity halogen bulb (MI-150).

Electrode Preparation and for Photo-electrochemical Measurements

The chromoionophore I/PPP micro-droplet array on a BPPG electrode was achieved by deposition of a stock solution (10 cm^3 acetonitrile, 80 mg PPP, and the required mass of chromoionophore I, plus 10 μL $HClO_4$ 70 wt%) and evaporation. Typically, a 5 μL aliquot of this solution was deposited by pipette on to the electrode surface to provide a 40 nL volume final deposit of randomly arranged micro-droplets. The electrode was cleaned after each set of experiments by rinsing with acetonitrile and re-polishing with fine silicon carbide paper.

Acknowledgement

S.A. thanks the HEC Pakistan for financial support. F.M. thanks the EPSRC and the NSF for supporting the project "Microphase Photo-Electrochemistry: Light Driven Liquid-Liquid Ion Transfer Processes and Two-Phase Micro-Photovoltaic Systems" (EP/G002614/1). We thank the EPSRC UK National Electron Paramagnetic Resonance Service at The University of Manchester.

References

[1] V.V. Cosofret, E. Lindner, R.P. Buck, R.P. Kusy, J.Q. Whitley, *J. Electroanal. Chem.* **1993**, *345*, 169-181.

[2] V.V. Cosofret, E. Lindner, T.A. Johnson, M.R. Neuman, *Talanta* **1994**, *41*, 931-938.

[3] Y. Qin, E. Bakker, *Talanta* **2002**, *58*, 909-918.

[4] M. Bochenska, *J. Inclusion Phenomena Mol. Recog. Chem.* **1995**, *22*, 269-275.

[5] M.J. Ruedas-Rama, E.A.H. Hall, *Analyst*, **2006**, *131*, 1282-1291.

[6] I.H.A. Badr, *Anal. Lett.* **2001**, *34*, 2019-2034.

[7] W.H. Chan, A.W.M. Lee, J.Z. Lu, *Anal. Chim. Acta*, **1998**, *361*, 55-61.

[8] A.R. Firooz, M. Movahedi, A.A. Ensafi, *Sens. Actuators B-Chem.* **2012**, *171*, 492-498.

[9] J.W. Zhu, J.Y. Zhai, X. Li, Y. Qin, *Sens. Actuators B-Chem.* **2011**, *159*, 256-260.

[10] I. Tsagkatakis, S. Peper, R. Retter, M. Bell, E. Bakker, *Anal. Chem.* **2001**, *73*, 6083-6087.

[11] A. Ulianas, L.Y. Heng, M. Ahmad, *Sensors*, **2011**, *11*, 8323-8338.

[12] I. Tsagkatakis, S. Peper, E. Bakker, *Anal. Chem.* **2001**, *73*, 315-320.

[13] J. Langmaier, E. Lindner, *Anal. Chim. Acta*, **2005**, *543*, 156-166.

[14] B. Kovacs, G. Nagy, R. Dombi, K. Toth, *Biosens. Bioelectron.* **2003**, *18*, 111-118.

[15] M.S. Alqasaimeh, L.Y. Heng, M. Ahmad, *Sensors*, **2007**, *7*, 2251-2262.

[16] T.M. Nahir, R.P. Buck, *Helv. Chim. Acta,* **1993**, *76*, 407-415.

[17] S. Bodor, J.M. Zook, E. Lindner, K. Toth, R.E. Gyurcsanyi, *Analyst*, **2008**, *133*, 635-642.

[18] A.M. Kelly, N. Katif, T.D. James, F. Marken, *New J. Chem.* **2010**, *34*, 1261-1265.

[19] F. Marken, R.D. Webster, S.D. Bull, S.G. Davies, *J. Electroanal. Chem.*, **1997**, *437*, 209-218.

[20] C.E. Banks, T.J. Davies, R.G. Evans, G. Hignett, A.J. Wain, N.S. Lawrence, J.D. Wadhawan, F. Marken, R.G. Compton, *Phys. Chem. Chem. Phys.*, **2003**, *5*, 4053-4069.

[21] J.D. Wadhawan, R.G. Compton, F. Marken, S.D. Bull, S.G. Davies, *J. Solid State Electrochem.*, **2001**, *5*, 301-305.

[22] J.D. Wadhawan, A.J. Wain, A.N. Kirkham, D.J. Walton, B. Wood, R.R. France, S.D. Bull, R.G. Compton, *J. Amer. Chem. Soc.*, **2003**, *125*, 11418-11429.

[23] J.D. Wadhawan, A.J. Wain, R.G. Compton, *ChemPhysChem*, **2003**, *4*, 1211-1215.

[24] F. Marken, J.D. Watkins, A.M. Collins, *Phys. Chem. Chem. Phys.*, **2011**, *13*, 10036-10047.

[25] A.M. Collins, X.H. Zhang, J.J. Scragg, G.J. Blanchard, F. Marken, *ChemPhysChem*, **2010**, *11*, 2862-2870.

[26] A.M. Collins, G.J. Blanchard, J. Hawkett, D. Collison, F. Marken, *Langmuir*, **2011**, *27*, 6471-6477.

[27] K. Sugawara, Y. Yamauchi, S. Hoshi, K. Akatsuka, F. Yamamoto, S. Tanaka, H. Nakamura, *Bioelectrochem. Bioenergetics*, **1996**, *41*, 167-172.

[28] F. Ni, H. Feng, L. Gorton, T.M. Cotton, *Langmuir*, **1990**, *6*, 66-73.

[29] T. Sagara, S. Igarashi, H. Sato, K. Niki, *Langmuir*, **1991**, *7*, 1005-1012.

[30] S. Ahmed, I.A.I. Hassan, H. Roy, F. Marken, *J. Phys. Chem. C*, **2013**, *117*, 7005-7012.

[31] L.M. Peter, *J. Solid State Electrochem.*, **2013**, *17*, 315-326.

[32] J. Krysa, J. Jirkovsky, O. Bajt, G. Mailhot, *Catal. Today*, **2011**, *161*, 221-227.

[33] *Handbook of Chemistry and Physics*, 74th ed., D.R. Lide, CRC Press, London, 1994, p. 8-46.

[34] D. Schaming, M. Hojeij, N. Younan, H. Nagatani, H.J. Lee, H.H. Girault, *Phys. Chem. Chem. Phys.*, **2011**, *13*, 17704-17711.

[35] G.G. Wallace, C.O. Too, D.L. Officer, P. Dastoor, *MRS Bull.*, **2005**, *30*, 46-49.

[36] Y.J. Zhang, T.Y. Mori, L. Niu, J.H. Ye, *Energy Environ. Sci.*, **2011**, *4*, 4517-4521.